ISSN 1070-3284, Russian Journal of Coordination Chemistry, 2017, Vol. 43, No. 7, pp. 481–490. © Pleiades Publishing, Ltd., 2017.

Syntheses, Structural Determination, and Binding Studies of Binuclear Nine-Coordinate $(MnH)_4[Ho_2^{III}(Dtpa)_2] \cdot 12H_2O$ and Polynuclear Nine-Coordinate $\{(MnH)[Ho^{III}(Egta)] \cdot 3H_2O\}_n$[1]

F. Y. Tian, F. Yang, X. Q. Jiang, Q. Wu, and J. Wang*

Department of Chemistry, Liaoning University, Shenyang, 110036 P.R. China

**e-mail: wangjuncomplex890@126.com*

Received April 25, 2016

Abstract—Two novel rare earth metal coordination compounds, $(MnH)_4[Ho_2^{III}(Dtpa)_2] \cdot 12H_2O$ (**I**) (Mn = methylamine, H_5Dtpa = diethylenetriamine-*N*,*N*,*N*',*N*'',*N*''-pentaaceticacid) and $\{(MnH)[Ho^{III}(Egta)] \cdot 3H_2O\}_n$ (**II**) (H_4Egta = ethyleneglycol-bis(2-aminoethylether)-*N*,*N*,*N*',*N*'-tetraacetic acid) have been successfully synthesized through direct heating reflux and characterized by FT-IR spectroscopy, thermal analysis, and single-crystal X-ray diffraction techniques (CIF files CCDC nos. 890878 (**I**) and 1457061 (**II**)). Complex **I** shapes a binuclear nine-coordinate structure with distorted tricapped trigonal prismatic conformation and crystallizes in the triclinic crystal system with space group $P\bar{1}$. The central Ho^{3+} ion is coordinated by three nitrogens and six oxygens from two octadentate Dtpa ligands. The cell dimensions are as follows: $a = 9.8420(10)$, $b = 12.1319(13)$, $c = 13.2931(15)$ Å, $\alpha = 89.223(2)°$, $\beta = 68.4280(10)°$, $\gamma = 72.1280(10)°$ and $V = 1396.0(3)$ Å^3. Complex **II** adopts a polynuclear nine-coordinate structure with pseudo-monocapped square antiprismatic conformation and crystallizes in the monoclinic crystal system with space group $C2/c$. The central Ho^{3+} ion is coordinated by two nitrogens and seven oxygens from two octadentate Egta ligands. The crystal data are as follows: $a = 38.4755(13)$, $b = 13.5569(5)$, $c = 8.7343(3)$ Å, $\beta = 100.135(3)°$ and $V = 4484.8(3)$ Å^3.

Keywords: Ho(III) complex, nine-coordination, synthesis, determination, Dtpa and Egta ligands

DOI: 10.1134/S1070328417070089

INTRODUCTION

Rare-earth metal complexes have increasingly been a research focus in different multidisciplinary area [1–4]. For example, Tb(III) and Eu(III) complexes are generally used as fluorescence probe in diagnosing certain diseases, light emitting diode (LED), biological sensors, lasers materials, and electroluminescent devices [5–9]. $^{153}Sm(III)$ have been widely used for tumor therapy of brain, liver, lung, heart, and bone tissues due to half-life of 46.27 h and β- and γ-emissions with moderate energy [10–12]. Many Gd(III) complexes have been used as contrast agents for magnetic resonance imaging (MRI) diagnoses because of seven high-spin single electrons in *f*-orbits [13, 14]. Dy(III) complexes have antibacterial activities and reduce blood sugar levels for their desirable physical characteristics and availability [15–18]. $^{166}Ho^{3+}$ ion can emit appropriate rays, thus, the $^{166}Ho(III)$ complexes have been adopted to diagnose and treat various tumors [19, 20]. Therefore, it is necessary to determine the crystal and molecular structures of rare-earth metal complexes.

In general, rare earth metal ions can form high-coordinate complexes, such as eight-, nine-, and ten-coordinate complexes, with various aminopolycarboxylic acid ligands [21–23]. The structures and coordination numbers of rare-earth metal compound with aminopolycarboxylic acid generally depend on the ionic radius and electrons configuration as well as counter ion. For example, for triethylenetetramine-*N*,*N*,*N*',*N*'',*N*''',*N*'''-hexaacetic acid (H_6Ttha) ligand, La^{3+}, Ce^{3+}, Pr^{3+}, and Nd^{3+} ions with big ionic radii and less *f*-orbital electrons form ten-coordinate complexes [24–26]. Tm^{3+}, Yb^{3+}, and Lu^{3+} ions with small ionic radii and many *f*-orbital electrons form eight-coordinate complexes [27, 28]. And the Sm^{3+}, Eu^{3+}, Gd^{3+}, Er^{3+}, and Ho^{3+} ions, in the intermediate states of lanthanide(III), only form nine-coordinate complexes [29, 30]. The same regularity can also be used in the rare-earth metal ions with other aminopolycarboxylic acid. However, it is not absolute. Due to the different ligands, for the same rare-earth metal ion its coordinate structures generally show markedly different characters.

In general, Ho^{3+} shapes mononuclear structure with nine-coordinate distorted tricapped trigonal pris-

[1] The article is published in the original.

matic conformation, such as $(EnH_2)_{1.5}[Ho^{III}(Ttha)] \cdot 4.5H_2O$ and $(EnH_2)[Ho^{III}(Egta)(H_2O)]_2 \cdot 6H_2O$ [31]. Moreover, we should also research the influence of methylamine (Mn) as counter ion on the molecular structures of Ho^{3+} complexes with H_5Dtpa and H_4Egta ligands. In order to get deeper insight into the influence, two Ho(III) complexes with H_5Dtpa and H_4Egta ligands, $(MnH)_4[Ho_2^{III}(Dtpa)_2] \cdot 12H_2O$ (**I**) and $(MnH)[Ho^{III}(Egta)] \cdot 3H_2O$ (**II**), were successfully synthesized, respectively, and characterized by FT-IR spectroscopy, thermal analysis, and single-crystal X-ray diffraction techniques. As expected, **I** and **II** are both nine-coordinate, but the coordinate structure, molecular structure, and crystal structure are all different. That is, they take distorted tricapped trigonal prismatic conformation and pseudo-monocapped square antiprismatic conformation, respectively. This study demonstrates again that the structures of rare-earth metal complexes with aminopolycarboxylic acid are mainly determined by ionic radii, ligand shape, and counter ion.

EXPERIMENTAL

Materials and methods. Ho_2O_3 powder (99.999%, Yuelong Rare Earth Co., Ltd., China) and ligands H_4Egta and H_5Dtpa (A.R., Beijing SHLHT Science and Trade Co., Ltd., China) were used to synthesize the title aminopolycarboxylic acid complexes. In addition, Mn aqueous solution was used to adjust the pH of above Ho^{3+} and Dtpa or Egta mixed solutions to 6.0.

Synthesis of I. H_5Dtpa (1.965 g, 5.0 mmol) was added to 100 mL warm water and Ho_2O_3 powder (0.9446 g, 2.5 mmol) was added to the above solution slowly. The solution became transparent after the mixture had been stirred and refluxed for 15.0 h. And then the pH value was adjusted to 6.0 by dilute Mn aqueous solution. Finally, the solution was concentrated to 25 mL. A white crystal appeared after seven weeks at room temperature. The yield is 2.29 g (78.96%). The composition and structure of **I** were detected by thermal analyzer (XT-V130, Beijing Xinzhou, Company, China) and X-ray diffractometer (SMART CCD type, Bruker Company, Germany).

Synthesis of II. H_4Egta (1.9017 g, 5.0 mmol) was added to 100 mL warm water and Ho_2O_3 powder (0.9446 g, 2.5 mmol) was slowly added to the above solution. After the mixture had been stirred and refluxed for 18.0 h, the solution became transparent. The pH value was adjusted to 6.0 by dilute Mn aqueous solution. Finally, the solution was concentrated to 25 mL and put at static environment. A white crystal appeared after eight weeks at room temperature. The yield is 2.37 g (83.55%). (The composition and structure of of **II** were detected by thermal analyzer and X-ray diffractometer same as for the synthesis of **I**).

X-ray structure determination. X-ray intensity data of **I** and **II** were collected on a Bruker SMART CCD type X-ray diffractometer system withgraphite-monochromatized MoK_α radiation ($\lambda = 0.71073$ Å) using φ–ω scan technique in the range of $1.72° \le \theta \le 26.00°$. Their structures were solved by direct methods. All non-hydrogen atoms were refined anisotropically by full matrix least-squares methods on F^2. All the calculations were performed by the SHELXTL-97 program on PDP11/44 and Pentium MMX/166 computers. The crystal data and structure refinement for two complexes were listed in Table 1. The selected bond distances and bond angles of two complexes were listed in Table 2. And some selected hydrogen bond distances and hydrogen bond angles of two complexes were listed in Table 3.

Supplementary material has been deposited with the Cambridge Crystallographic Data Centre (nos. 890878 (**I**) and 1457061 (**II**); deposit @ccdc.cam.ac.uk or http://www.ccdc.cam.ac.uk).

RESULTS AND DISCUSSION

The comparsion of FT-IR spectra between H_5Dtpa and complex **I** are shown in Figs. 1a and 1b. It reveals that the ν(C–N) of **I** appears at 928 cm^{-1}, which displays rea-shifts by 33 cm^{-1} compared with that (961 cm^{-1}) of the ligand H_5Dtpa. The ν_{as}(COO) of **I** appears at 1622 cm^{-1}, while the ν_{as}(COO) of H_5Dtpa appears at 1635 cm^{-1}, so complex **I** displays red-shifts by 13 cm^{-1}. The ν_s(COO) of **I** appears at 1401 cm^{-1}, which displays a slight blue-shift by 4 cm^{-1} compared with that (1397 cm^{-1}) of H_5Dtpa. These shifts confirmed that the carboxylic oxygen atoms of the H_5Dtpa ligand are coordinated to the Ho^{3+} ion. Furthermore, the characteristic broad absorption peaks of hydroxy group appears at 3446 cm^{-1}. This suggests that there is H_2O molecule exists in **I**, coordinating to the Ho^{3+} ion. The contrast of FT-IR spectra between H_4Egta and complex **II** are shown in Figs. 1c, 1d). It displays that the ν(C–N) of complex **II** appears at 1094 cm^{-1}, which displays rea-shifts by 41 cm^{-1} compared with that (1135 cm^{-1}) of the H_4Egta ligand. It indicates that the amine nitrogen atoms of H_4Egta ligand are coordinated to the Ho^{3+} ion. The ν_{as}(COO) of H_4Egta at 1745 cm^{-1} disappears in the FT-IR spectrum of **II**. But in the FT-IR spectrum, the ν_{as}(COO) of **II** can be found at 1625 cm^{-1}, indicating a red-shift by 100 cm^{-1}. And the ν_s(COO) of **II** appears at 1425 cm^{-1}, which displays a blue-shift (20 cm^{-1}) compared with 1405 cm^{-1} of the H_4Egta ligand. These shifts suggest that oxygens in the carboxylic group participate in coordination to Ho^{3+} ion. Moreover, there is a strong and wide absorption peak around 3434 cm^{-1} in

Table 1. Crystallographic data and structure refinement details for complexes **I** and **II**

Parameter	Value	
	I	**II**
Empirical formula	$C_{32}H_{84}Ho_2N_{10}O_{32}$	$C_{15}H_{32}HoN_3O_{13}$
Formula weight	1450.95	627.37
Temperature, K	293(2)	293(2)
Crystal system	Triclinic	Monoclinc
Space group	$P\bar{1}$	$C2/c$
Unit cell dimensions:		
a, Å	9.8420(10)	38.4755(13)
b, Å	12.1319(13)	13.5569(5)
c, Å	13.2931(15)	8.7343(3)
α, deg	89.223(2)	
β, deg	68.4280(10)	100.135(3)
γ, deg	72.1280(10)	
Volume, Å^3	1396.0(3)	4484.8(3)
Z	1	8
ρ_{calcd}, Mg/m^3	1.726	1.858
Absorption coefficient, mm^{-1}	2.912	7.232
F(000)	736	2512
Crystal size, mm	0.40 × 0.32 × 0.30	0.20 × 0.11 × 0.06
θ Range for data collection, deg	2.56–25.02	3.46–66.18
Limiting indices	$-11 \le h \le 11$, $-7 \le k \le 14$, $-15 \le l \le 15$	$-38 \le h \le 45$, $-15 \le k \le 16$, $-10 \le l \le 10$
Reflections collected	7107	13906
Independent reflections (R_{int})	4825 (0.0359)	3935 (0.0486)
Completeness to θ_{max}, %	97.9	100.0
Max and min transmission	0.4753 and 0.3887	0.6708 and 0.3257
Goodness-of-fit on F^2	1.079	1.037
Final R indices ($I > 2\sigma(I)$)	$R_1 = 0.0432$, $wR_2 = 0.1056$	$R_1 = 0.0368$, $wR_2 = 0.0933$
R indices (all data)	$R_1 = 0.0602$, $wR_2 = 0.1189$	$R_1 = 0.0458$, $wR_2 = 0.0994$
Largest difference peak and hole, e Å^{-3}	2.376 and −1.510	1.565 and −0.957
Absorption correction	Semi-empirical	

the FT-IR spectrum of complex **II**, which could be reasonably assigned to O–H stretching vibrations.

As shown in Fig. 2a, the TG curve of complex **I** can be divided into three stages. The first stage of weight loss is about 9.0% from room temperature to 140°C, which corresponds to loss of MnH. From 140 to 220°C, the changes of weight is very small. This suggests that complex **I** is correspondingly stable in the range of this temperature. The second stage of weight loss of 15.0% from 220 to 302°C should correspond to the release of the crystal water. The third stage of weight loss is attributed to the decomposition and combustion of the carboxylate starting from 302 to 800°C, and the corresponding weight loss ratio is about 47.0%. The final residue is mainly the mixture of Ho_2O_3 and $Ho_2(CO_3)_3$, and the overall weight loss is about 71.0%.

As shown in Fig. 2b, the thermal decomposition process of complex **II** can also be divided into three stages. The first stage of weight loss is about 10.25% from room temperature to 140°C, which corresponds to loss of MnH. From 140 to 400°C, the second stage of weight loss of 16.0% should correspond to the release of the crystal water. The third stage of weight

Table 2. Selected bond distances (Å) and angles (deg) of complexes **I** and **II***

Bond	*d*, Å	Bond	*d*, Å	Bond	*d*, Å
		I			
Ho(1)–O(1)	2.387(5)	Ho(1)–O(5)	2.329(5)	Ho(1)–N(1)	2.626(6)
Ho(1)–O(2)$^{\#1}$	2.414(5)	Ho(1)–O(7)	2.336(5)	Ho(1)–N(2)	2.602(6)
Ho(1)–O(3)	2.300(5)	Ho(1)–O(9)	2.388(5)	Ho(1)–N(3)	2.626(6)
		II			
Ho(1)–O(1)	2.495(3)	Ho(1)–O(4)$^{\#2}$	2.343(3)	Ho(1)–O(9)	2.336(3)
Ho(1)–O(2)	2.475(3)	Ho(1)–O(5)	2.372(3)	Ho(1)–N(1)	2.626(3)
Ho(1)–O(3)	2.287(3)	Ho(1)–O(7)	2.339(3)	Ho(1)–N(2)	2.598(4)
Angle	ω, deg	Angle	ω, deg	Angle	ω, deg
		I			
O(1)Ho(1)O(2)$^{\#1}$	70.95(16)	O(3)Ho(1)O(9)	72.98(18)	O(7)Ho(1)O(2)$^{\#1}$	72.44(16)
O(1)Ho(1)O(9)	88.64(16)	O(3)Ho(1)N(1)	64.02(18)	O(7)Ho(1)O(9)	90.20(17)
O(1)Ho(1)N(1)	61.83(16)	O(3)Ho(1)N(2)	88.02(19)	O(7)Ho(1)N(1)	137.41(18)
O(1)Ho(1)N(2)$^{\#1}$	129.99(17)	O(3)Ho(1)N(3)	69.81(18)	O(7)Ho(1)N(2)	74.75(18)
O(1)Ho(1)N(3)	142.86(18)	O(5)Ho(1)O(1)	87.92(16)	O(7)Ho(1)N(3)	66.98(17)
O(2)$^{\#1}$Ho(1)N(1)	124.11(16)	O(5)Ho(1)O(2)$^{\#1}$	79.42(17)	O(9)Ho(1)O(2)$^{\#1}$	72.17(17)
O(2)$^{\#1}$Ho(1)N(2)	138.26(19)	O(5)Ho(1)O(7)	75.16(17)	O(9)Ho(1)N(1)	131.09(18)
O(2)$^{\#1}$Ho(1)N(3)	118.45(17)	O(5)Ho(1)O(9)	150.92(18)	O(9)Ho(1)N(2)	133.05(17)
O(3)Ho(1)O(1)	78.74(17)	O(5)Ho(1)N(1)	71.04(18)	O(9)Ho(1)N(3)	63.97(17)
O(3)Ho(1)O(2)$^{\#1}$	133.71(18)	O(5)Ho(1)N(2)	67.71(17)	N(2)Ho(1)N(1)	68.97(18)
O(3)Ho(1)O(5)	134.24(18)	O(5)Ho(1)N(3)	128.28(17)	N(2)Ho(1)N(3)	69.23(18)
O(3)Ho(1)O(7)	136.72(17)	O(7)Ho(1)O(1)	141.85(17)	N(3)Ho(1)N(1)	117.16(18)
		II			
O(1)Ho(1)N(1)	67.33(11)	O(3)Ho(1)N(2)	131.83(12)	O(7)Ho(1)O(4)$^{\#2}$	149.50(11)
O(1)Ho(1)N(2)	132.18(12)	O(4)$^{\#2}$Ho(1)O(1)	68.28(11)	O(7)Ho(1)O(5)	76.53(11)
O(2)Ho(1)O(1)	67.01(11)	O(4)$^{\#1}$Ho(1)O(2)	74.06(11)	O(7)Ho(1)N(1)	74.07(11)
O(2)Ho(1)N(1)	123.10(11)	O(4)$^{\#2}$Ho(1)O(5)	133.88(11)	O(7)Ho(1)N(2)	65.16(12)
O(2)Ho(1)N(2)	67.80(12)	O(4)$^{\#1}$Ho(1)N(1)	116.68(11)	O(9)Ho(1)O(1)	138.40(11)
O(3)Ho(1)O(1)	95.77(11)	O(4)$^{\#2}$Ho(1)N(2)	112.68(12)	O(9)Ho(1)O(2)	101.51(12)
O(3)Ho(1)O(2)	150.19(11)	O(5)Ho(1)O(1)	71.98(11)	O(9)Ho(1)O(4)$^{\#2}$	70.13(12)
O(3)Ho(1)O(4)$^{\#2}$	76.97(10)	O(5)Ho(1)O(2)	69.52(11)	O(9)Ho(1)O(5)	143.96(11)
O(3)Ho(1)O(5)	130.14(10)	O(5)Ho(1)N(1)	65.45(10)	O(9)Ho(1)O(7)	82.45(12)
O(3)Ho(1)O(7)	83.28(11)	O(5)Ho(1)N(2)	78.43(11)	O(9)Ho(1)N(1)	135.29(12)
O(3)Ho(1)O(9)	74.73(11)	O(7)Ho(1)O(1)	137.56(11)	O(9)Ho(1)N(2)	66.18(11)
O(3)Ho(1)N(1)	65.29(10)	O(7)Ho(1)O(2)	126.05(11)	N(2)Ho(1)N(1)	130.52(12)

* Symmetry codes: $^{\#1}$ $-x+1, -y+1, -z+1$ for (**I**). $^{\#1}$ $x, -y, z+1/2$; $^{\#2}$ $x, -y, z-1/2$ for (**II**).

loss is attributed to the decomposition and combustion of the carboxylate starting from 400 to 800°C, and the weight loss ratio is about 44.65%. The final residue is mainly the mixture of Ho_2O_3 and $Ho_2(CO_3)_3$, and the overall weight loss is about 70.9% for **II**.

As seen from Fig. 3a, each Ho^{3+} ion is surrounded by three amine N atoms (N(1), N(2), and N(3)) and six carboxylic O atoms (O(1), O(2), O(3), O(5), O(7), and O(9)), and they all come from two adjacent H_5Dtpa ligands. The three N atoms and five O atoms

Table 3. Geometric parameters of hydrogen bonds of complexes **I** and **II**

D–H···A	Distance, Å			Angle DHA, deg	Symmetry code
	D–H	H···A	D···A		
			I		
N(4)–H(4*A*)···O(14)	0.89	2.18	2.909(2)	139	$x, y + 1, z$
N(4)–H(4*A*)···O(11)	0.89	2.59	3.108(2)	117	$-x + 1, -y + 1, -z + 1$
N(4)–H(4*B*)···O(7)	0.89	2.00	2.876(3)	168	
N(4)–H(4*B*)···O(8)	0.89	2.47	3.118(2)	129	
N(4)–H(4*C*)···O(6)	0.89	1.92	2.809(3)	175	$-x + 1, -y + 2, -z + 1$
N(5)–H(5*A*)···O(9)	0.89	1.99	2.878(3)	176	$-x + 1, -y + 1, -z + 1$
N(5)–H(5*B*)···O(10)	0.89	1.90	2.784(2)	172	$x + 1, y, z$
N(5)–H(5*C*)···O(5)	0.89	2.17	2.923(2)	141	
N(5)–H(5*C*)···O(1)	0.89	2.38	2.950(2)	121	$-x + 1, -y + 1, -z + 1$
			II		
N(3)–H(3*A*)···O(7)	0.89	1.99	2.871(2)	168	$-x + 1, y, -z + 1/2$
N(3)–H(3*B*)···O(10)	0.89	1.89	2.749(2)	172	
N(3)–H(3*C*)···O(9)	0.89	1.96	2.825(3)	163	$-x + 1, -y, -z + 1$

of one H_5Dtpa ligand form seven five-membered chelating rings with the central Ho^{3+} ion, in which the five atoms are almost coplanar in each ring. It must point out that complex **I** is biunclear nine-coordinate geometry with distorted tricapped trigonal prismatic conformation (Fig. 4a). In the coordinate atoms around Ho^{3+} ion, the set of N(2), O(5), O(7) and the set of O(1), O(3), O(9) form two appxoimate parallel trigonal (top and bottom) planes, respectively, forming a trigonal prism. The O(2)$^{\#}$, N(1), and N(3) atoms are above the three approximately quadrangular planes formed by O(1), O(5), O(7), O(9), and O(1), O(3), O(5), N(2), and O(3), O(7), O(9), N(2) shaping three capped positions, respectively. The total angles of N(3)Ho(1)O(2), O(2)Ho(1)N(1) and N(1)Ho(1)N(3) are 359.718°, close to 360°, indicating that the O(2)$^{\#}$, N(1), and N(3) atoms lie in the same plane. In addition, from Fig. 4a, the value of the square antiprism angle can be calculated for the O(3), O(1), O(5), and N(2) square plane. The average value of the trigonal dihedral angle between Δ(N(2)O(3)O(1)) and Δ(O(3)O(1)O(5)) is about 7.921°, and between Δ(O(5)N(2)O(1)) and Δ(N(2)O(1)O(3)) is about 8.429°. For the O(9), O(2), O(7), and N(3) square plane, the value of the dihedral angle between Δ(N(3)O(7)O(9)) and Δ(O(7)O(9)O(2)) triangles is about 19.42°, and between Δ(O(9)N(3)O(7)) and Δ(N(3)O(7)O(2)) triangles is about 24.96°. According to these calculated data, both are smaller than 26.4°, we can confirmedly conclude that the conformation of $Ho(1)N_3O_6$ in the $[Ho_2^{III}(Dtpa)_2]^{4-}$ complex anion indeed keeps adistorted tricapped trigonal prismatic conformation.

Furthermore, as seen from Table 2, the average value of the Ho(1)–O bond distances is 2.359(5) Å. In contrast, the average value of the Ho(1)–N bond distances is 2.618(5) Å. From the above data we can draw a conclusion that the Ho(1)–O bonds are much stable than Ho(1)–N bonds. We can also find that a series of bond angles for understanding the coordination structure. The reason might be that the O(1) atom forms hydrogen bond with the adjacent crystal water molecule. According to these data, we can firmly conclude that the conformation around Ho(1) indeed keeps a distorted tricapped trigonal prismatic conformation.

The results given in this paper and the ones reported previously indicated that the Ho^{3+} ion can form nine-coordinate complexes with aminopolycarboxylic acids due to the ionic radius of 1.041 Å and electronic configuration of f^{10} and all chelating rings are five-membered rings in the coordination structure. In the previous studies, we reported the synthesis and structures of $(NH_4)_3[Ho^{III}(Ttha)] \cdot 5H_2O$. It was found that the Ho^{3+} ion adopts a nine-coordinate mononuclear structure [32]. In this paper, we use MnH^+ as a counter ion to interact with the $[Ho_2^{III}(Dtpa)_2]^{4-}$ complex anion, yielding complex **I**. However, the Ho^{3+} ion adopts a nine-coordinate binuclear structure in **I**. Therefore, we can make forecast that for the same rare-earth metal ion their coordinate structures may show markedly different characters due to the different ligands.

It can be seen from Fig. 5a that there are two molecules of complex **I** in a unit cell. The complex molecules connect with another one throughhydrogen bonds and electrostatic forces with crystal water and

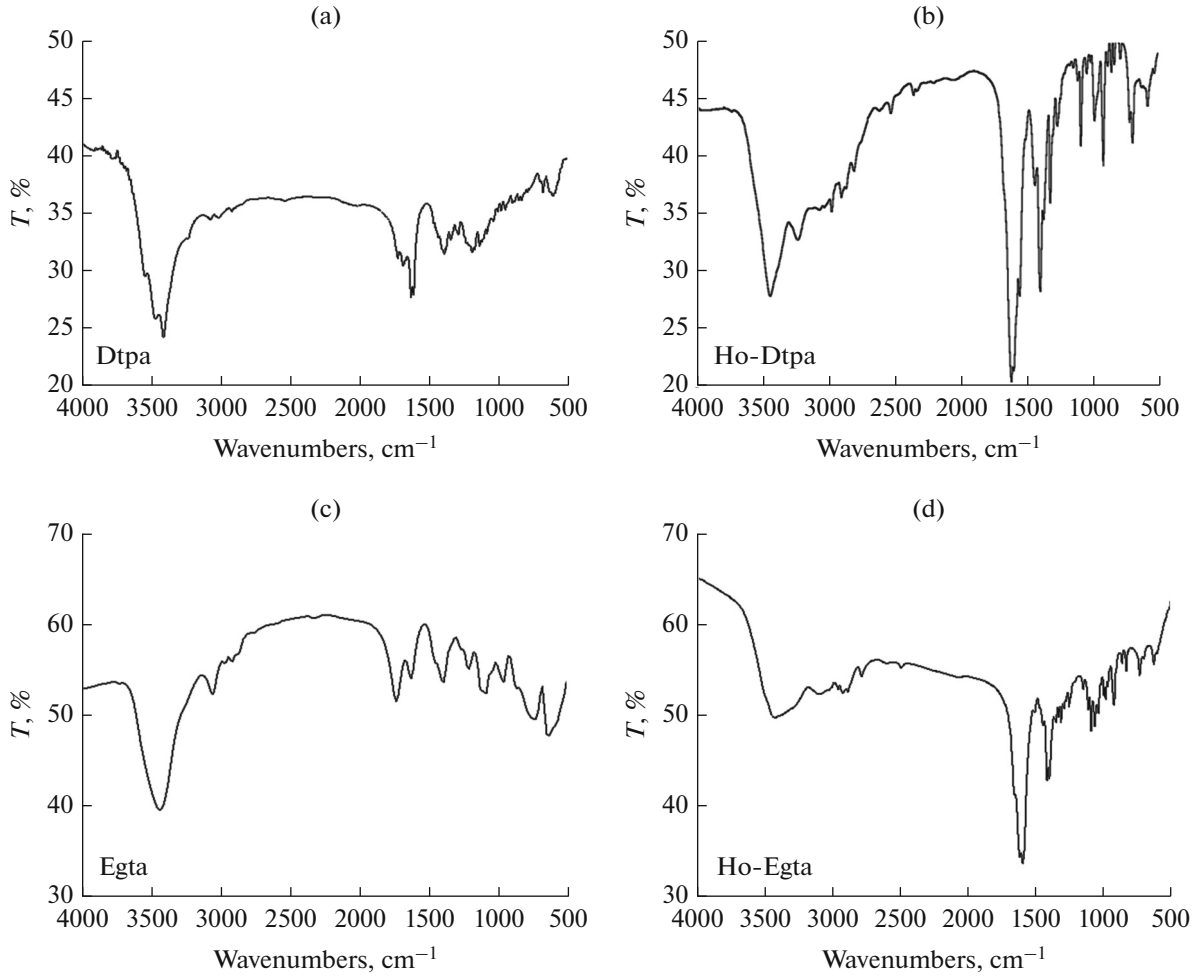

Fig. 1. Infrared spectra of H_5Dtpa (a), **I** (b), H_4Egta (c) and **II** (d).

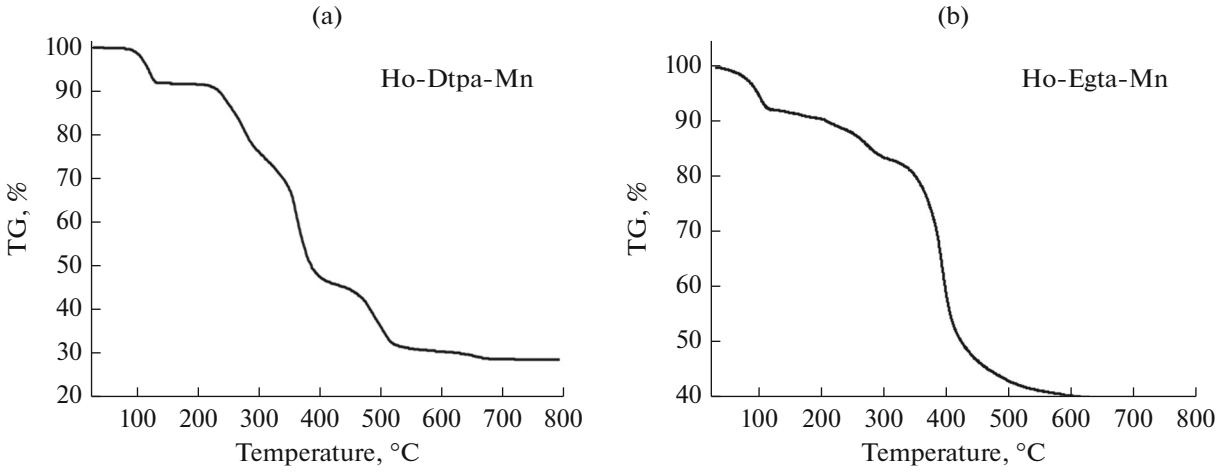

Fig. 2. TG curve of **I** (a) and **II** (b).

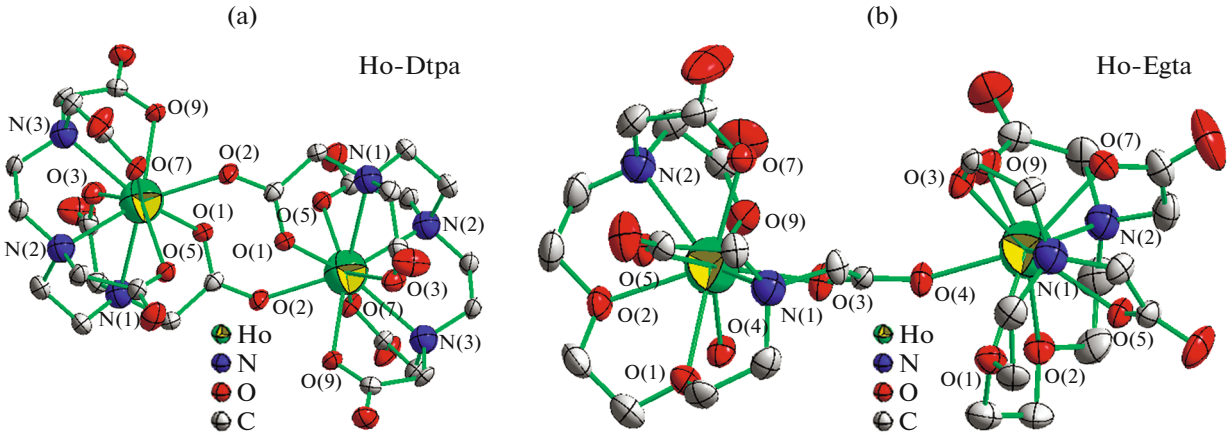

Fig. 3. Molecular structures of **I** (a) and **II** (b).

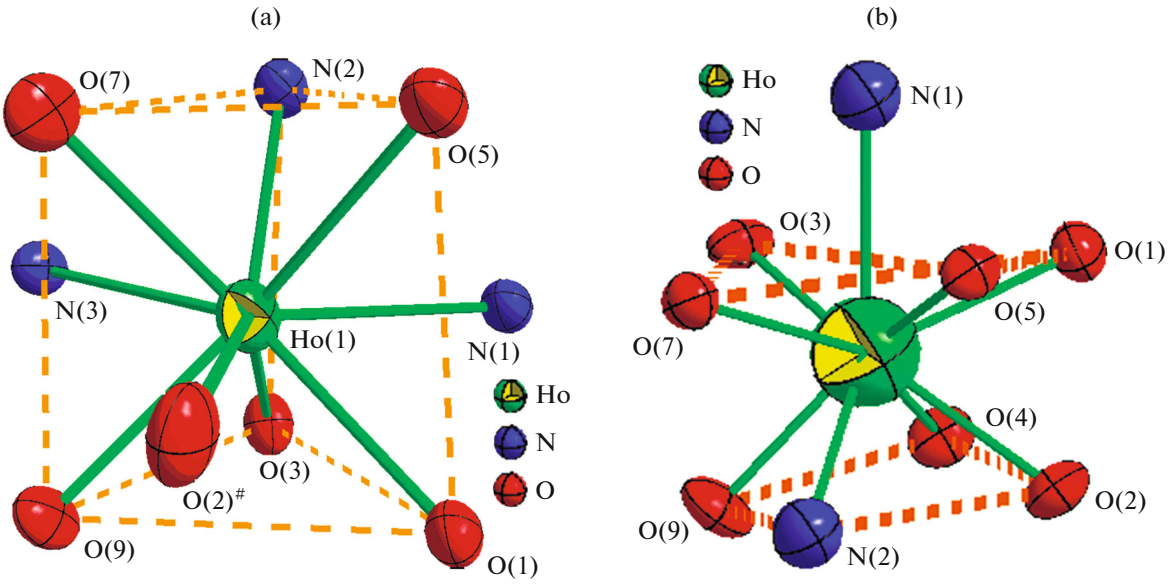

Fig. 4. Coordination polyhedrons around Ho^{3+} ion in **I** (a) and **II** (b).

protonated cation (MnH^+). As seen from Fig. 6a, there are two type of MnH^+ cations. The first type of MnH^+ cation forms hydrogen bonds with two $[Ho_2^{III}(Dtpa)_2]^{4-}$ complex anion. N(4) of the MnH^+ cation links three O atoms (O(6), O(7), and O(14)), that is one uncoordinated carboxyl atom O(6) and one coordinated carboxyl atom O(7) from two different $[Ho_2^{III}(Dtpa)_2]^{4-}$ complex anion and the O(14) atom from one crystal water. The second MnH^+ cation which is highly symmetric, forms hydrogen bonds with two adjacent $[Ho_2^{III}(Dtpa)_2]^{4-}$ complex anion. The N(5) atom of the second MnH^+ cation connects with three uncoordinated carboxyl O atoms (O(1), O(5), and O(9)), which come from two neighboring $[Ho_2^{III}(Dtpa)_2]^{4-}$ complex anions, respectively. That is, O(1) and O(9) atoms come from the same $[Ho_2^{III}(Dtpa)_2]^{4-}$ complex anion, while the O(5) atom come from another one.

Every two $[Ho_2^{III}(Dtpa)_2]^{4-}$ complex anions are interconnected together by sharing the first type of methylamine (N(4)–C(15)) along *x* axis, forming a basic secondary building unit (SBU). The bond lengths of N(4)–O(6) and N(4)–O(7) are 2.809 and 2.876 Å, respectively. The two adjacent SBU are further connected by sharing the second type of methylamine along *x* axis with N(5)–O(1), N(5)–O(5), N(5)–O(9), and N(5)–O(10) bond lengths of 2.950, 2.923, 2.878, and 2.784 Å, respectively, resulting in the

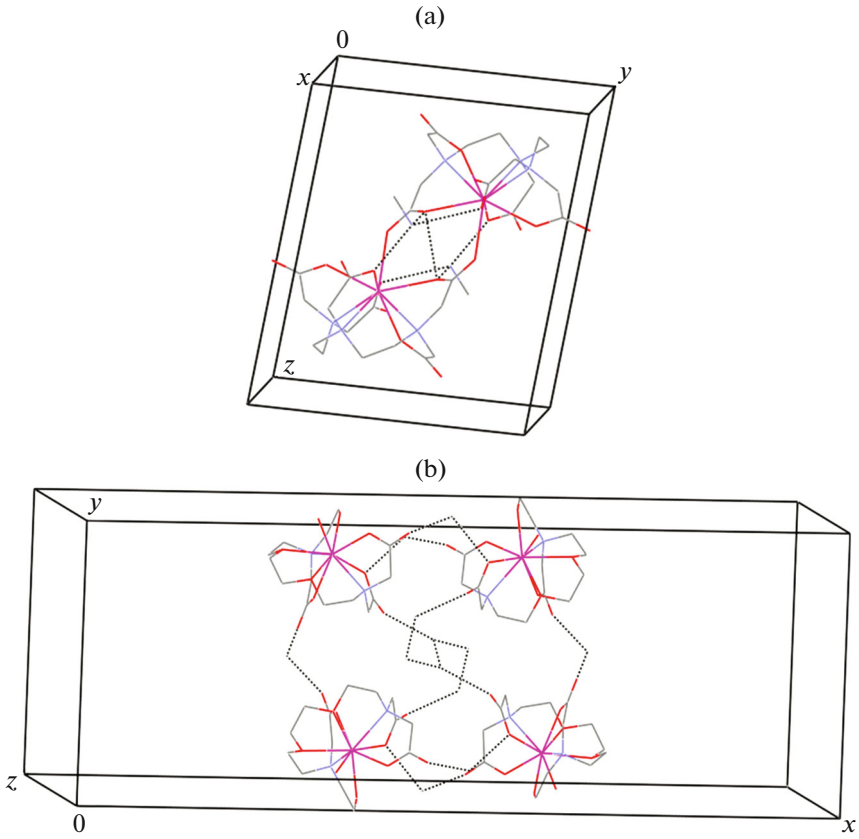

Fig. 5. Arrangements of complexes **I** (a) and **II** (b) in unit cell (dashed lines represent intermolecular hydrogen bonds).

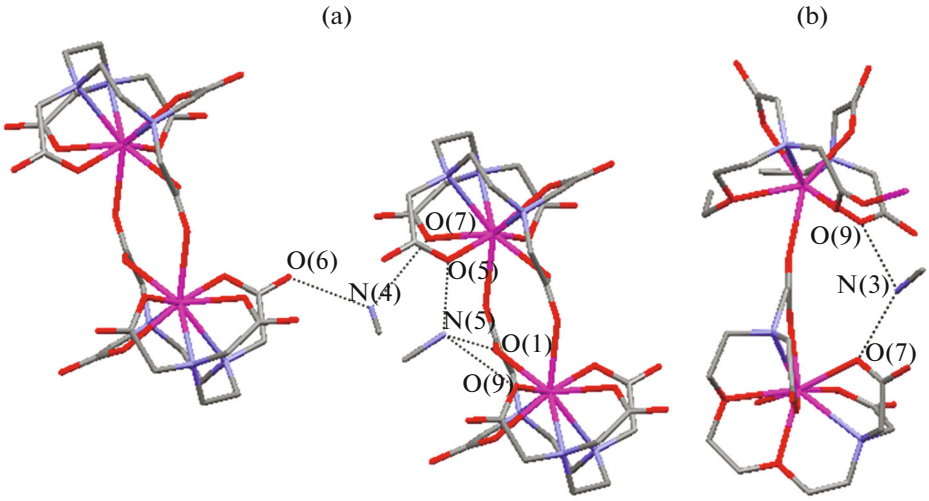

Fig. 6. Bindings between MnH_4^+ and $[Ho_2^{III}(Dtpa)_2]^{4-}$ in **I** (a) and MnH_4^+ and $[Ho^{III}(Egta)]^-$ in (**II**) (b) (dashed lines represent intermolecular hydrogen bonds).

formation of infinite 1D chain by *x* axis. The two 1D chains are formed along *xy* plane.

As shown in Fig. 3b, it can be seen that the nine-coordinated structure of complex **II** is a 1 : 1 proportion of rare earth metal ions to ligand stoichiometry. The central Ho^{3+} ion is coordinated with two N atoms and seven O atoms, of which one O atom (O(4)) belongs to a coordinated water molecule. The remain-

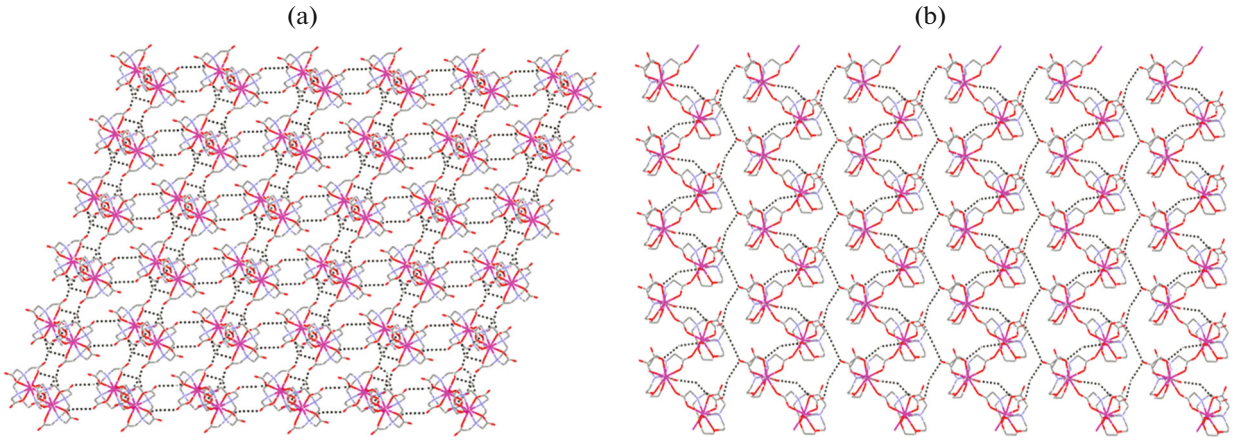

Fig. 7. Polyhedral view of the 1D ladder-like layered network of **I** (a) and **II** (b).

ing two amine N atoms and four carboxyl O atoms and two methylamine atoms all belong to one octadentate H_4Egta ligand. Like complex **II**, the eight atoms also shape seven structurely stable five-member ring with the central Ho^{3+} ion and the five atoms in each five-member ring are almost coplanar.

Apparently, the coordination geometry around the central Ho^{3+} ion in $[Ho^{III}(Egta)]^-$ complex anion is a nine-coordinate pseudo-monocapped square antiprism with the capping position occupied by one amine atom N(1). The top quadrilateral plane of antiprism is formed by four carboxyl O atoms (O(1), O(3), O(5), and O(7)). The bottom quadrilateral plane is done by one amine atom N(2), one coordinate water atom O(4), and two carboxyl atoms O(2) and O(9). The distorted angle of the two (top and bottom) quadrilateral planes is about 48.88°, which accords with the prismatic geometry.

The series of bond distances for complex **II** are given in Table 2. The average value Ho(1)–O bond lengths is 2.378(3) Å, while the average value Ho(1)–N bond lengths is 2.612(3) Å. In any case, the Ho(1)–O bonds are more stable than the Ho(1)–N bonds.

In addition, as seen from Fig. 4b, it can be found that, to the above square plane, the value of the dihedral angle between Δ(O(1)O(3)O(5)) and Δ(O(1)O(3)O(7)) is about 9.262°, and between Δ(O(1)O(5)O(7)) and Δ(O(3)O(5)O(7)) is about 10.049°. To the bottom square plane, the value of the dihedral angle between Δ(O(2)O(4)N(2)) and Δ(O(9)O(4)N(2)) is about 8.981°, and between Δ(O(2)O(9)N(2)) and Δ(O(2)O(9)O(4)) is about 8.1°. In view of these calculated data, we can draw a conclusion that the conformation of $Ho(1)N_2O_7$ in $[Ho^{III}(Egta)]^-$ complex anion indeed keeps a pseudo-monocapped square antiprism.

As shown in Fig. 5b, there are four molecules of complex **II** in a unit cell. The complex molecules connect with one another through hydrogen bonds and electrostatic forces with crystal water and protonated methylamine cations (MnH^+). As seen from Fig. 6b, the cation is located in a center of symmetric structure and the symmetric center is in the middle position of the methylamine. Each methylamine cation (MnH^+) forms hydrogen bonds with two neighboring $[Ho^{III}(Egta)]^-$ complex anions. That is, every N(3) connects two O atoms (O(7) and O(9)), in which O(7) and O(9) come from two carboxylic groups of two $[Ho^{III}(Egta)]^-$ complex anion, respectively. The distances of N(3)–O(7) and N(3)–O(9) are 2.871 and 2.825 Å, respectively. As shown in Fig. 7b, every two $[Ho^{III}(Egta)]^-$ complex anions are interconnected together by sharing methylamine (N(3)–C(15)–C(15)–N(3)), forming a basic SBU, the two neighboring SBU are connected resulting in the formation of 2D network in plane. Owing to the special coordination environment, the Newman' pattern dihedral angle of Mn is closely to 180°. So four atoms of Mn locate in the same plane. Therefore, it can be observed that amino acids as a part of protein can interact with $[Ho^{III}(Egta)]^-$ complex anion through different binding manner.

ACKNOWLEDGMENTS

The authors greatly acknowledge the National Science Foundation of China (21371084 and 31570154), Key Laboratory Basic Research Foundation of Liaoning Provincial Education Department (L2015043), Liaoning Provincial Department of Education Innovation Team Projects (LT2015012), and Youth Science Foundation of Liaoning University (2013LDQN14) for financial support. The authors also thank our colleagues and other students for their participating in this work.

REFERENCES

1. Bünzli, J.C.G. and Piguet, C., *Chem. Rev.*, 2002, vol. 102, p. 1897.
2. Tsukube, H. and Shinoda, S., *Chem. Rev.*, 2002, vol. 102, p. 2389.
3. Sabbatini, N., Guardigli, M., and Lehn, J.M., *Coord. Chem. Rev.*, 1993, vol. 123, p. 201.
4. Snejko, N., Cascales, C., Lor, B.G., et al., *Chem. Commun.*, 2002, vol. 13, p. 1366.
5. Desa, G.F., Malter, O.L., Donege, C.D., et al., *Coord. Chem. Rev.*, 2000, vol. 196, p. 300.
6. Sirimanne, P.M. and Cheng, Y.B., *J. Lumin.*, 2009, vol. 129, p. 563.
7. Stanimirov, S. and Petkov, I., *Spectrochim. Acta, A*, 2009, vol. 72, p. 1127.
8. Robinson, M.R., O'Regnan, M.B., and Bazzan, G.C., *J. Chem. Soc., Chem. Commun.*, 2000, p. 1645.
9. Kido, J. and Okamoto, Y., *Chem. Rev.*, 2002, vol. 102, p. 2357.
10. Pana, T.M., Lina, J.C., Wub, M.H., et al., *Biosens. Bioelectron.*, 2009, vol. 24, p. 2864.
11. Neves, M., Gano, L., Pereira, N., et al., *Nucl. Med. Biol.*, 2002, vol. 29, p. 329.
12. Lauffer, R.B., *Chem. Rev.*, 1987, vol. 87, p. 901.
13. Aime, S., Botta, M., Fasano, M., et al., *Chem. Soc. Rev.*, 1998, vol. 27, p. 19.
14. Chen, Z.J. and Liu, X.L., *Rare Earths*, 2001, vol. 22, p. 68.
15. Kremer, C., Torres, J., Dominguez, S., et al., *Coord. Chem. Rev.*, 2005, vol. 249, p. 567.
16. Volkert, W.A., Goeckeler, W.F., Ehrhardt, G.J., et al., *J. Nucl. Med.*, 1991, vol. 32, p. 174.
17. Li, W.P., Ma, D.S., Higginbotham, C., et al., *Nucl. Med. Biol.*, 2001, vol. 28, p. 145.
18. Lee, T.H., Cho, Y.H., Lee, J.D., et al., *Immunol. Lett.*, 2006, vol. 106, p. 19.
19. Chen, J.Q., Linder, K.E., and Cagnolini, A., *Appl. Radiat. Isotopes*, 2008, vol. 66, p. 497.
20. Wang, J., Wang, Y., Zhang, Zh.H., et al., *J. Coord. Chem.*, 2006, vol. 59, p. 295.
21. Wang, J., Gao, G.R., Wang, X.F., et al., *J. Coord. Chem.*, 2008, vol. 61, p. 220.
22. Wang, J., Zhang, X.D., Zhang, Y., et al., *Russ. J. Coord. Chem.*, 2004, vol. 30, p. 850.
23. Wang, J., Zhang, X.D., Zhang, Y., et al., *J. Struct. Chem.*, 2004, vol. 45, p. 144.
24. Wang, R.Y., Li, J.R., Jin, T.Zh., et al., *Polyhedron*, 1997, vol. 16, p. 2037.
25. Kim, Ch.H. and Lee, S.G., *Bull. Korean Chem. Soc.*, 1999, vol. 16, p. 417.
26. Chen, Y., Ma, B.Q., Liu, Q.D., et al., *Inorg. Chem. Commun.*, 2000, vol. 3, p. 319.
27. Wang, R.Y., Zhang, H.J., and Jin, T.Zh., *Chem. J. Chin. Univ.*, 1999, vol. 20, p. 176.
28. Liu, B., Gao, J., Wang, J., et al., *Russ. J. Coord. Chem.*, 2009, vol. 35, p. 422.
29. Liu, B., Hu, P., Wang, J., et al., *Russ. J. Coord. Chem.*, 2009, vol. 35, p. 758.
30. Mondry, A. and Starynowicz, P., *Dalton. Trans.*, 1998, vol. 3, p. 859.
31. Bai, Y.Gao. Wang, J., et al., *Russ. J. Coord. Chem.*, 2013, vol. 39, p. 147.
32. Wang, X.F., Liu, X.Zh., Wang, J., et al., *Russ. J. Coord. Chem.*, 2008, vol. 34, p. 135.